ELSEVIER

BioSystems 67 (2002) 147–156

BioSystems

www.elsevier.com/locate/biosystems

Noise-induced divisive gain control in neuron models

André Longtin [a,*], Brent Doiron [a,b], Adi R. Bulsara [c]

[a] Department of Physics, University of Ottawa, 150 Louis Pasteur, Ottawa, Ont., Canada K1N 6N5
[b] Department of Cellular and Molecular Medicine, University of Ottawa, Ottawa, Ont., Canada K1H 8M5
[c] SPAWAR Systems Center Code D363, 49590 Lassing Road, RM A341, San Diego, CA 92152-6147, USA

Accepted 22 August 2002

Abstract

A recent computational study of gain control via shunting inhibition has shown that the slope of the frequency-versus-input (f–I) characteristic of a neuron can be decreased by increasing the noise associated with the inhibitory input (Neural Comput. 13, 227–248). This novel noise-induced divisive gain control relies on the concommittant increase of the noise variance with the mean of the total inhibitory conductance. Here we investigate this effect using different neuronal models. The effect is shown to occur in the standard leaky integrate-and-fire (LIF) model with additive Gaussian white noise, and in the LIF with multiplicative noise acting on the inhibitory conductance. The noisy scaling of input currents is also shown to occur in the one-dimensional theta-neuron model, which has firing dynamics, as well as a large scale compartmental model of a pyramidal cell in the electrosensory lateral line lobe of a weakly electric fish. In this latter case, both the inhibition and the excitatory input have Poisson statistics; noise-induced divisive inhibition is thus seen in f–I curves for which the noise increases along with the input I. We discuss how the variation of the noise intensity along with inputs is constrained by the physiological context and the class of model used, and further provide a comparison of the divisive effect across models.

Keywords: Neuron models; Integrate and fire; Theta-neuron; Noise; Gain control; Inhibition; Shunting

1. Introduction

Many neurons are thought to perform scaling operations on their input over a variety of time scales (Koch, 1999; Carandini and Heeger, 1994; Nelson, 1994; Salinas and Thier, 2000). This scaling results from changes in the frequency-versus-input current (f–I) characteristic of a cell. For example, if the slope of this f–I curve is high, a small slow variation in input current is mapped by the cell into a larger variation in instantaneous firing rate. One commonly assumed fast-acting mechanism involves gain control through shunting inhibition, i.e. through a conductance G_s with a reversal potential V_s near the resting potential V_r of the cell. Since $V_s \approx V_r$, the current $I_s = G_s (V - V_s)$ contributed by this conductance will be small despite the fact that a large inhibitory input can increase G_s substantially. However, the main effect

* Corresponding author. Tel.: +1-613-562-5800x6762; fax: +1-613-562-5190
E-mail address: alongtin@physics.uottawa.ca (A. Longtin).

0303-2647/02/$ - see front matter
PII: S0303-2647(02)00073-4

of this kind of inhibition, which is classically mediated by $GABA_A$ type channels, is through the increase of the total cell conductance, i.e. the reduction of the input resistance and thus of the membrane time constant τ; this smaller τ then decreases the effect of excitatory input, whether due to an injected current input or to synaptic input.

It had long been believed that shunting inhibition could be used to 'scale' or 'divide' input by altering the slope of the f–I curve. This hope was guided by the fact that membrane voltage does relate to input current in a divisive manner in the subthreshold regime (Ohm's law); consequently, increasing total conductance via an increase in shunting inhibition decreases the slope of the V–I curve. However, Holt and Koch (1997) showed that, when a cell fires, shunting inhibition causes a shift of the f–I curve to higher input currents, yet the slope of the f–I curve remains unchanged. This is a consequence of the resetting of the voltage following spikes, which qualitatively alters the relation between voltages and currents averaged over short times.

In a recent paper, Doiron et al. (2001a) have found that noise associated with inhibitory synaptic input causes a decrease in slope in the f–I characteristic of model pyramidal cells at lower frequencies, rather than a shift. The compartmental ionic model was built from anatomical and physiological data from a pyramidal cell of the electrosensory lateral line lobe of the weakly electric fish Apteronotus Leptorhynchus (Berman and Maler, 1999). The frequencies where this 'noise-induced divisiveness' (NID) was found were relevant to the normally behaving fish. In an independent experimental study, NID was also observed in the context of balanced excitatory and inhibitory synaptic inputs (Chance et al., 2002). The inclusion of noise in the gain control problem thus revealed a feedforward mechanism for divisive gain control at the single cell level. The noise arose naturally from simulations of the inhibitory synaptic input on the compartmental model using the program NEURON. An even simpler leaky integrate-and-fire (LIF) model showing the effect was

$$C\frac{dV}{dt} = -[\bar{g} + \sigma(\bar{g})\eta(t)]V + I \quad (1)$$

where $\eta(t)$ was lowpass-filtered Gaussian white noise (of zero mean and unit variance) added to the mean conductance $\bar{g}$. It is meant to represent the mean total inhibitory input in the compartmental model. The reversal potential for this input has been set to zero, a good approximation for shunting inhibition. Also, σ is the standard deviation of the fluctuations in $\bar{g}$, and depends on $\bar{g}$. Note also that in general, $\bar{g}$ includes all conductances, but we have focussed only on the inhibitory one for simplicity. The correlation time of this Ornstein–Uhlenbeck noise was matched to that of the mean total conductance fluctuations observed in the full compartmental model; these fluctuations were the result of inhibitory synaptic activity distributed across the dendrites and soma. The noise on the total conductance was necessary to obtain sigmoidally increasing f–I curves, as seen experimentally and in the compartmental model. f–I curves for increasing mean levels of inhibition $\bar{g}$ simply shifted rightwards (as in Holt and Koch, 1997) if the noise intensity σ^2 was independent of the mean inhibition, i.e. subtractive gain control occurred. However, if σ^2 was increased monotonically with $\bar{g}$, as expected for Poisson inhibitory inputs, divisive gain control was observed at lower frequencies, with subtractive behavior at higher frequencies.

The NID effect can be quantified using the average slope of the f–I curve (see Doiron et al., 2001a), which can be simply determined as the ratio of some interval of mean firing frequencies (e.g. 0–40 Hz) divided by the corresponding range of input currents. Due to the statistical nature of the f–I curves with noise, some criterion must be used to define these lower and upper frequency bounds (especially the lower one which in principle is never zero with finite noise and has a large variance). The essence of the NID effect was that the denominator of this ratio increases. This occurs in spite of the fact that the f–I curve shifts to the right for higher inhibition; this is because the increased noise makes firings appear for relatively lower values of input current. Note also that the actual f–I curve is sigmoidal, yet it

can be adequately approximated by a linear curve at lower frequencies, at least for the purpose of quantifying NID simply.

In this paper we consider how shunting inhibition interacts with Gaussian white noise to modify the f–I characteristic in simple standard neuron models that approximate more accurate Hodgkin–Huxley type models. The first goal is to assess the generality of the NID. This is useful in particular if one wishes to model networks of cells performing this novel kind of gain control. It is also useful to identify the key ingredients of this effect, and how they may interact with other aspects of stochastic firing activity. Our paper also considers how the effect occurs in the same large-scale model used in Doiron et al. (2001a) in which the input parameter is the rate of arrival of excitatory inputs, rather than a constant bias current. This involves extending the model to include synaptic excitatory inputs. This part of our study examines what happens when the noise level automatically increases along with the rate of excitatory inputs (as expected for Poisson processes), which is even closer to the physiological situation.

We have emphasized so far that the noise is mainly related to synaptic activity. In particular, when a pre-synaptic cell increases its firing rate, the total conductance of the postsynaptic cell increases, and thus its membrane time constant decreases. All but one of the four models studied in our paper include this effect on the conductance. It is informative nevertheless to see that the NID effect does not require that this conductance change, as will be illustrated in the next section on the standard LIF model which is still widely used. On the other hand, we will find that an increase in the noise intensity along with the level of inhibitory input is necessary for the effect in all models.

The particular physiological context and phenomenon under study will motivate the choice of a given model. This choice however will constrain the way in which noise can be made input-dependent. This issue is nicely discussed in a recent study of gain control in the presence of synaptic inputs, where it is argued that one can focus specifically on two factors, the ratio of inhibition to excitation, and the total current equal to excitatory minus inhibitory contributions (Lánský and Sacerdote, 2001). That study considered models without synaptic reversal potentials. Our study focusses strongly on models with synaptic reversal potentials, and can thus be seen as complementary to it in many aspects. Also, in a given experiment, it may be possible and desirable to vary the bias using intracellular injected current, and for this reason we include this current in the total current along with synaptic inputs. For all models studied here, we discuss the choices available for varying noise with input, and due to lack of space, focus on one reasonable choice to study noisy gain control. Our goal is to determine if and how each model can exhibit NID, since these models are used in a variety of contexts on a variety of cells.

Section 2 analyzes noise-induced divisive inhibition in the standard LIF model with additive Gaussian white noise. In Section 3, the effect is studied in an LIF model with inhibitory synaptic input and reversal potentials. Section 4 considers how the effect arises in a simple one-dimensional model, known as the theta-neuron, that has a saddle-node bifurcation to periodic firing (paradigm of type I membrane). Section 5 studies the effect in a large-scale compartmental model (Doiron et al., 2001a) in which the f–I curves are computed for increasing frequency of excitatory inputs, rather than increasing I as in Doiron et al. (2001a). The paper closes with a discussion of results and an outlook onto future research.

2. Leaky integrate-and-fire: additive noise

The LIF models focusses simply on the effect of currents on neuron firing activity. Since LIF models replace real action potentials by a simple voltage reset condition following a threshold crossing, they account for the effects of non-spiking currents on firings, in contrast to the fast currents such as the sodium and delayed rectifier currents that generally underlie action potential generation. With additive noise, it can be used to describe the response to a noisy injected current, or to stochastic synaptic input in a first approximation. This latter approximation is good if the subthreshold voltage fluctuations are far away

from inhibitory and excitatory reversal potentials, or when the synaptic conductance is small compared with the total membrane conductance without synaptic input (see e.g. Koch, 1999, Chapter 1; Tuckwell, 1989).

The noise of interest here is Gaussian white noise, following the usual approximation for synaptic input in the diffusion limit where the rates $\mu_{e,i}$ of arrival of postsynaptic potentials (PSPs) go to infinity and their amplitudes $a_{e,i}$ go to 0. The total driving current can be written as $a_e\mu_e - a_i\mu_i + I$ where I is some external applied current (e.g. via an electrode). In this form, the equation is of course an approximation since the input is partly synaptic, yet the synaptic conductances do not multiply battery terms of the form $V - V_{rev}$ as they normally would; yet the equation has more 'biophysical detail' than the standard LIF model which lumps all inputs into the parameter I.

The first passage time density for this Ornstein–Uhlenbeck process cannot be solved analytically except when the steady state coincides with the threshold. However, it is possible to obtain the mean FPT in terms of quadratures. One can then compute f–I curves from this formalism for varying degrees of inhibition. More precisely, we consider

$$C\frac{dV}{dt} = -gV + \mu + \sigma\xi(t) \tag{2}$$

where we have written $\mu \equiv I + a_e\mu_e - a_i\mu_i$, and as usual the intensity of the Gaussian white noise $\sigma\xi(t)$ is $\sigma^2 \equiv 2D$. Bulsara et al. (1996) have derived a relatively simple expression for the first passage time density (Z) for this process in terms of μ, using the method of images ($C = 1$):

$$G(t) = \frac{2a\, e^{-gt}}{\sqrt{2\pi\alpha^3}}\left(g\alpha + \frac{\dot{\alpha}}{2}\right)e^{-w^2} + \frac{\dot{\psi}}{2}[1 + \Phi(z)] \tag{3}$$

where

$$\alpha(t) = \frac{D}{g}(1 - e^{-2gt}) \tag{4}$$

$$\beta(t) = \frac{\mu}{g}(1 - e^{-gt}) \tag{5}$$

$$z = \frac{a - 2a\, e^{-gt} - \beta(t)}{\sqrt{2\alpha}} \tag{6}$$

$$w = \frac{a - e^{-gt} - \beta(t)}{\sqrt{2\alpha}} \tag{7}$$

$$\psi(t) = \frac{2a}{\alpha(t)}[-a + \beta(t) + ae^{-gt}]e^{-gt}$$

$$\Phi(z) = \frac{2}{\sqrt{\pi}}\int_0^z e^{-y^2}\, dy \tag{8}$$

i.e. $\Phi(z)$ is the error function. This expression is approximate, and its accuracy increases as the (deterministic) asymptotic voltage μ/g approaches the threshold value (it is exact when both are equal to one another). As we explore the behavior of this model around this boundary between the subthreshold and suprathreshold regimes, this approximation is acceptable.

In computing an f–I characteristic for this model with increasing inhibition, we are immediately confronted with choices, as for all models studied in our paper (see Introduction). First, what exactly is varying when the 'I' in 'f–I' is increasing? One possibility is to assume that only the injected current I increases, keeping μ_e and μ_i constant; curves for different inhibition levels can then be obtained using different (positive) values of μ_i. The noise intensity σ^2 then does not change with I, but just stays at some chosen value meant to represent baseline noise. This somewhat trivial case will amount to shifting the f–I curves rightward as μ_i increases. Alternately, one can increase σ along with μ_i. Yet another possibility is to increase μ_e instead of I, for a given level of inhibition μ_i (and keeping I fixed); the f–I curve then reflects how the mean firing rate changes with increasing frequency of excitatory synaptic inputs. In that case again, one must decide how σ varies with μ_e and μ_i.

In this section we conform to the standard simplified picture in which the f–I curve for the LIF is obtained for increasing injected current I, for different values of μ_i (i.e. different levels of inhibition), keeping $\mu_e = 0$ for all simulations. Further, σ does not increase with I (which is approximately true for injected current), but does

increase with μ_i (which is true for synaptic current); we have set $\sigma(\mu) = a_i\sqrt{\mu_i}$), as expected in the diffusion approximation without reversal potentials (Tuckwell, 1989). As we will see, this will give us a baseline NID effect for an LIF model with additive Gaussian white noise. It does not account for the change in total conductance as μ_i changes, as is the case for LIF models without reversal potentials (Lánský and Sato, 1999). The dynamics are then:

$$\frac{dV}{dt} = -gV + I - a_i\mu_i + \sigma(\mu_i)\xi(t) \quad (9)$$

Fig. 1 shows three f–I curves from this model for three levels of inhibition (μ_i). It is seen that the slope of the f–I curve in the lower frequency range decreases as μ_i increases, i.e. NID is seen. Further, at higher mean output firing rates, the curves appear simply shifted to the right as μ_i increases (subtractive inhibition). If the noise intensity σ^2 had not been increased along with the rate of shunting inhibition μ_i, the curves would then be purely shifted versions of one another, without slope changes (not shown). This increase in σ^2 is thus crucial to seeing the NID effect in this model. Note that the absolute refractory period was set equal to zero for this model. For a positive absolute refractory period, subtractive inhibition at higher rates would still be seen, except that all the curves would then merge at high input levels.

The lower panel of Fig. 1 shows that slope of the f–I curve as a function of the level of inhibition. One sees a hyperbolic behavior, and the change in slope in stronger for the value of I above the deterministic threshold set at $I = 1$. In fact, the data can be fitted to a form $1/(x+a)^c$ (not shown) where a and c are constants that depend on the value of input at which the slopes are estimated. This form is close to pure divisive behavior ($1/x$), and it is in this sense that we use the term noise-induced divisive inhibition in our study. This applies also to the other models studied in our paper.

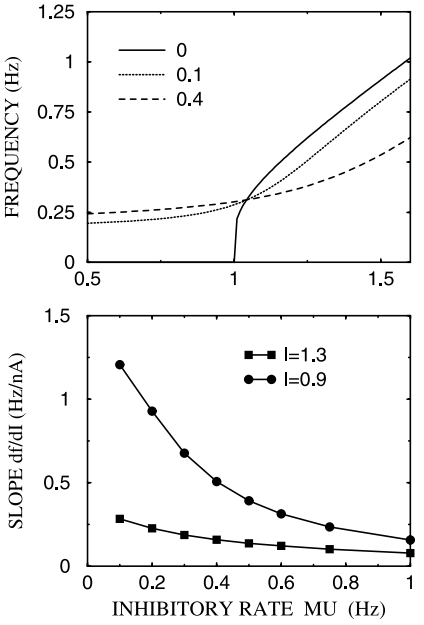

Fig. 1. Upper panel: Mean firing frequency reciprocal of Eq. (3) vs. input current from the analytical expression for the mean firing rate for the LIF model with additive Gaussian white noise Eq. (2), for three levels of inhibition (legend) $\mu_i = 0, 0.1, 0.4$; the corresponding noise levels are $D = 0.0, 0.0125, 0.05$. The $\mu = 0$ case is the control case without inhibition; the corresponding curve was calculated using the exact expression for the frequency of the deterministic LIF model. The slope of the f–I curve decreases with increasing inhibition over the lower frequency range, while a subtractive shift is seen at higher frequencies. Lower panel: Analytically determined slope of the f–I curves in the upper panel as a function of the level of inhibition, for two values of the input current ($I = 0.9$, subthreshold, and $I = 1.3$, suprathreshold). Parameters are $a = 1$ (threshold), $g = 1$, $a_i = 0.5$, $\mu_e = 0$ and $\sigma = a_i\sqrt{\mu_i}$. The absolute refractory period is zero, so the curves asymptote to linear non-saturating behavior.

3. Leaky integrate-and-fire: multiplicative noise

We now consider an LIF model where the rate of excitatory synaptic inputs is increased rather than I, and where the change in total conductance, i.e. the change in membrane time constant, resulting from this synaptic input is taken into account. It can be derived under certain assumptions from Stein's original model with reversal potentials (Lánská et al., 1994). It accounts for excitatory and inhibitory synaptic events, random variations in the amplitudes of these events, and reversal potentials. It has been devised in part because the

diffusion approximation applied to Stein's model with reversal potentials has a determistic diffusion limit, i.e. no noise is left in the diffusion approximation (Lánský and Lánská, 1987). These same authors have shown that randomness in the amplitudes, seen experimentally, allows for a noisy limit. We note that, at present, there does not seem to be a unique way to arrive at a Langevin equation in the diffusion approximation of Stein's model with reversal potentials and random EPSP and IPSP amplitudes (Lánská et al., 1994). We use the version described in Lánská et al. (1994):

$$\frac{dX(t)}{dt} = -\frac{X}{\tau} + \mu(V_E - X) + \nu(X - V_I) + \sigma\sqrt{(V_E - X)(X - V_I)}\xi(t) \quad (10)$$

The rate of arrival of EPSP's is given by λ; the EPSP amplitude is given by a mean value a plus a zero-mean random component A, $a\lambda = \mu$, and $\lambda E(A^2) = \sigma_A^2$ where E denotes the expectation value. The rate of arrival of IPSP's is given by ω; the IPSP amplitude is given by a mean value i plus a zero-mean random component I, $i\omega = v$ with $v < 0$ since $i < 0$, and $\omega E(I^2) = \sigma_I^2$. The noise intensity in Eq. (10) is thus defined as $\sigma^2 = \sigma_E^2 + \sigma_I^2$. Note the special 'multiplicative noise' form for the diffusion term. Lánský and Lánská (1987) have derived an analytical expression $E(T)$ for the expectation value of the interval T between firings for this model:

$$E(T) = \frac{1}{\beta}\sum_{n=0}^{\infty}\frac{(2\alpha/\sigma^2)_n}{(2\beta/\sigma^2 + 1)_n}\frac{S_t^{n+1} - y_o^{n+1}}{n+1} \quad (11)$$

where $(a)_n = a\,(a+1)(a+2)\ldots(a+n-1)$, $S_t = (S - V_I)/(V_E - V_I)$, S is the spiking threshold, $y_o = (x_o - V_I)/(V_E - V_I)$, x_o is the reset voltage after a spike, $\alpha = \tau^{-1} + \mu - v$ and $\beta = \mu - V_I/[\tau(V_E - V_I)]$. We have chosen to compute f–I curves by computing the reciprocal of $E(T)$ for increasing EPSP arrival rate λ, for a given rate of IPSP's ω. Parameters must also satisfy the following inequality in order that the reversal potentials V_E and V_I be inaccessible:

$$\sigma^2 < \frac{-2V_I}{\tau(V_E - V_I)} \quad (12)$$

Assuming for simplicity that $\sigma^2 = (\lambda + \omega)\varepsilon$, one can compute the variation of the noise intensity with the rate of EPSP's. This latter relationship for σ^2 can be made to satisfy Eq. (12) and the parameters used by Lánský and Lánská (1987) (their 'example 1') by using $\varepsilon = 0.0145$ (see caption of Fig. 2). The 'f–I' curves are shown in Fig. 2 for three frequencies of arrival of IPSP's. One clearly sees the decrease in slope as ω increases. Interestingly, for our chosen parameters, the curves do not shift much to the right with increasing inhibition, as seen e.g. in Figs. 3 and 4 for two models where the onset of repetitive firing occurs via a saddle-node bifurcation (this is based on numerical evidence for the model in Fig. 4). Rather, the gain control as seen in the decrease in slope is actually effective right around this bifurcation

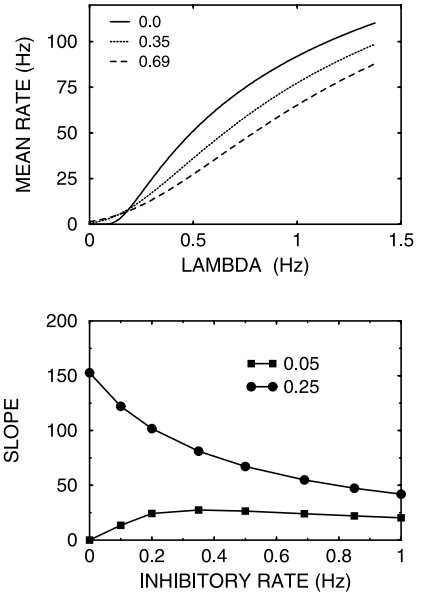

Fig. 2. Upper panel: Mean firing frequency vs. input current for the LIF model Eq. (10) obtained in the diffusion limit of the Stein model with reversal potentials and randomly varying EPSP and IPSP amplitudes; the analytical expression for this mean rate given by the reciprocal of Eq. (11) was used. The different levels of inhibition are controlled by the parameter ω shown in the legend. Lower panel: Slope of the curves in the upper panel as a function of inhibitory rate for two values of λ. Parameters are as in Lánská and Lánský (1994): example 1): $V_I = -10$ mV, $V_E = 100$ mV, $S = 10$ mV, $\tau = 5.8$ ms, $i = -0.2$, $a = 0.02$ and the reset voltage is $x_o = 0$. An absolute refractory period of 5 ms was included in the calculation.

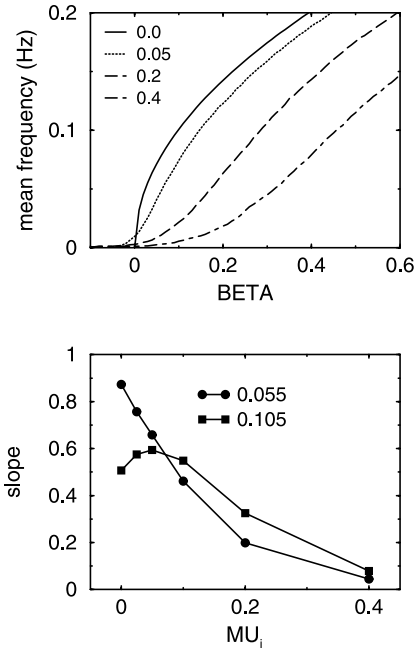

Fig. 3. Upper panel: Mean firing frequency vs. input current for the 'theta-neuron' model of type I membrane Eq. (13) . We have used $I=\beta-\mu_i$ and $\sigma^2=0.3125\mu_i$. Lower panel: Slope of the functions in the upper panel as a function of inhibitory rate μ_i, for two values of the bias β (see legend). Parameters are $\mu_i=0$ ($D=0$), $\mu_i=0.2$ ($D=0.03125$) and $\mu_i=0.4$ ($D=0.0625$). Mean firing rates were obtained at each value of β using five realizations of 2×10^5 time steps (one time step equals 0.01 s); the firing threshold was set at π. Slopes were estimated by first performing ten point running averages of the data in the upper panels, and then calculating their slope using a central difference scheme.

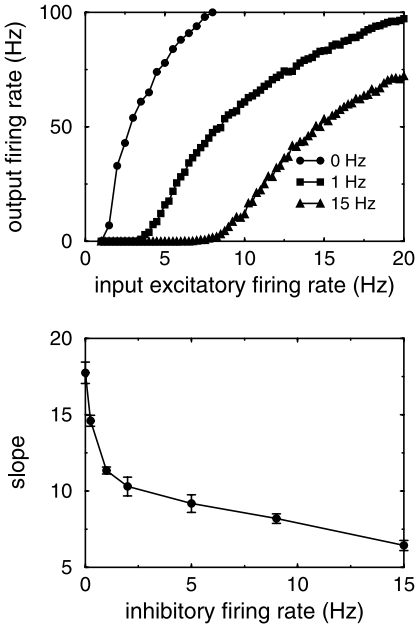

Fig. 4. Upper panel: Mean firing frequency vs. mean rate of arrival of excitatory synaptic input for the compartment model of a pyramidal cell (Doiron et al., 2001a), simulated using the program NEURON. Lower panel: estimated slope of the curves in the upper panel as a function of inhibitory firing rate. The slope was estimated using the slope of the chord between the point where the firing rate becomes non-zero to the point where it crosses 40 Hz. The input synaptic activity innervates the basal dendrites through 250 AMPA synapses distributed uniformly over the basal bush (distal input). The response of these synapses was modeled as an alpha function (Koch, 1999; Doiron et al., 2001a) with time constant 1.5 ms, reversal potential 0 mV (resting is -70 mV) and $g_{max}=0.5$ nS. The inhibitory drive was provided by 1000 $GABA_A$ synapses (shunting, i.e. reversal potential is also -70 mV) spread uniformly over the entire apical tree (proximal and distal) and the soma. The mean Poisson rates of these inhibitory synapses for each curve is indicated in the figure legend. The time constant for their alpha function was 7 ms, and $g_{max}=3$ nS. All synapses fired randomly with time intervals generated from an exponential distribution (Poisson input). An 'f–I' curve was generated by varying the rate of excitatory events from 1 to 20 Hz in intervals of 0.5 Hz, keeping the inhibitory rate fixed. Each mean firing rate was computed using 1000 ms simulation data, following a (discarded) 100 ms transient.

point. We also note in the lower panel that the presence of NID depends on the value of the excitatory input rate λ at which the slopes are calculated. For low λ, it is seen here that the slope goes through a maximum, instead of decaying in a hyperbolic manner. This maximum underlies the stochastic resonance effect in the model (Chialvo et al., 1997; see Section 6).

4. Theta-neuron

LIF models are useful to model the subthreshold dynamics, but totally disregard the actual spiking process. The effect of noise on ionic models with spiking currents and realistic repolarization mechanisms is thus of interest (see e.g. Brown et al., 1999 for a recent reference), as are studies on simplified versions of such ionic models that preserve some aspect of the spiking and reporalization dynamics (see e.g. Yu and Lewis, 1989; Longtin 2000 and references therein). One

such model is the so-called theta-neuron model (Ermentrout, 1996). It is derived from ionic models such as the Morris–Lecar model that have a transition to repetitive firing via a saddle-node bifurcation upon increasing a bias additive current. Its dynamics (on the circle) are governed by

$$\frac{d\theta}{dt} = 1 - \cos\theta + (1 + \cos\theta)(I + \sigma\xi(t)) \qquad (13)$$

where we have denoted the input to the cell by $I + \sigma\xi(t)$, $\xi(t)$ being Gaussian white noise as in Section 2. This noise is meant to represent all noise sources in the cell, especially synaptic noise (see also Gutkin and Ermentrout, 1998). It is an approximation to real synaptic input that accounts not only for the effect of such input on the mean bias but also on the total conductance of the cell (and thus on its time constant). The approximation gets better as the system approaches the saddle-node bifurcation, which occurs at $I = 0$. Here we study whether this model can exhibit the NID effect. In our experience so far, we suspect that it should, since its f–I curve has a sigmoidal shape in the presence of noise. Here we assume a hybrid version where $I \equiv \beta - \mu_i$, with β a constant bias that will vary as the abscissa in the f–I curve, and μ_i is the level of inhibition. We use the relationship for Poisson inputs $\sigma^2 = c\mu_i$ where c is a constant. Interestingly, this model also has a built-in refractory period, due to the finite time to go around the (circular) phase space back near the resting phase (resting voltage) following a spike. For this model, we have opted to use numerical simulations to obtain the f–I curve. Results are shown in Fig. 3, where it is again seen that the NID effect is present in this dynamical model, in a manner similar to the full compartmental model (that has a saddle-node bifurcation, Doiron et al., 2001b) studied in the next section.

5. Compartmental model of a pyramidal cell

In the original study of Doiron et al. (2001a), the NID effect was investigated using LIF models as well as a large scale compartmental model simulated using the NEURON package. In the latter case, the I in the f–I curve was simply the magnitude of an injected current. This is relevant to certain experimental settings, such as slice preparations. However, in the real system, the input is the mean rate of arrival of spikes at synapses, excitatory ones in particular (Berman and Maler, 1999). As is clear from the previous sections, an increase in excitatory input will also result in an increase in noise level. Here we study the NID effect using the rate of excitatory events instead of I. This is similar to an f–I curve, except that the noise on the input increases as the mean rate of Poisson inputs increases, and the same is true for the inhibitory activity (the same was true for the LIF model with reversal potentials studied above); this increase better mimicks the biophysical reality for uncorrelated synaptic inputs.

The model used in this section is the same as the one in Doiron et al. (2001a). Note that that model has been studied in great depth recently with respect to its novel bursting properties (Doiron et al., 2001b). For simplicity, the main current responsible for bursting (slowly inactivating K current) has been removed from our simulations. The result is a mode that mimicks well many known features of the real pyramidal cells, including the active and passive loading of the soma. The results are shown in Fig. 4, and are qualitatively similar to those shown in Doiron et al. (2001a). Thus the effect is expected to occur in the more realistic situation where 'input' is actually 'noisy synaptic input' whose intensity depends on the mean synaptic input. Note also that the simulation fully takes into account the decrease of the membrane time constant with increasing input strength.

6. Discussion

We have presented an analysis of the change of slope of f–I curves for increasing levels of inhibition in commonly used neuron models, as well as in a multicompartment model of a pyramidal cell with random synaptic input. It was found that the decrease in slope with increasing inhibition was a universal feature of all models studied. This was

true for both models with (Fig. 4) and without (Figs. 1–3) actual synaptic input; in fact the LIF models and the theta-neuron models studied here were all 'diffusive' approximations of neural dynamics with either injected and/or synaptic input. Only the full NEURON simulation (Fig. 4) actually included synaptic responses to discrete incoming spikes. The observed differences across models in the noise-induced divisive inhibition (NID) effect were more of a quantitative nature, and had most to do with the amount of rightward shift of the f–I curve upon increasing inhibition. This is true despite the fact that in some simulations the f–I curve was obtained by actually varying I, while in others, it was obtained by varying the rate of arrival of EPSP's (μ_e).

The NID effect was generally more pronounced for slopes measured above but near the deterministic onset of firing. Also, it was seen only if the noise level in the stochastic differential equation was increased along with the inhibition. If the noise intensity was kept fixed, the slopes of f–I curves for different levels of inhibition did not change significantly (not shown), as found in Doiron et al. (2001a) with colored noise on an LIF model. So to first order, the noise changes the gain (the slope), while inhibition generates a shift of the input-output function. However, a slope calculation on a complex model (Fig. 4) or on experimental data is more problematic, since the data are sparser and have inherent fluctuations. The slope can then be estimated as a chord (see Fig. 4 legend), which will depend mainly on noise, but also on the shift.

The similarity of the results in Figs. 3 and 4 also suggest that the precise bifurcation to repetitive spiking behavior, which both the compartmental model and the theta-neuron model share, may determine some aspect of the effect, such as the amount of shift. Those figures are also similar to our earlier results (Doiron et al., 2001a), including the LIF with additive colored noise; the correlation properties of the noise may thus also influence aspects such as the shift.

We have used analytical expressions for the mean firing rate for the LIF models with and without reversal potentials. It is nevertheless difficult to obtain analytical insight into the NID effect, due in great part to the complexity of the expressions. More analytical work would also be possible starting from other exact or approximate expressions for the mean firing rate (see e.g. Ricciardi, 1977; Tuckwell, 1989; Lánský and Sacerdote, 2001). The effect will depend quantitatively on the input level at which the slope is estimated, as we have shown.

This slope is an important characteristic for the encoding of slow subthreshold input signals (Yu and Lewis, 1989). It can be used to estimate the linear correlation between an input signal and the firing rate when the signal time scales are slower than the slowest neuron time scale (Chialvo et al., 1997). In fact, the range of input currents over which NID is seen overlaps the subthreshold regime where stochastic resonance (SR) occurs. For slow input signals to the LIF model, this effect is related to a maximization of this slope with increasing noise (Longtin, 2000; Chialvo et al., 1997). It is worth studying how NID affects the 'optimal noise' from the SR point of view. We expect that the slope of the f–I curve can in some cases still go through a maximum as a function of noise intensity; this is clearly seen in Fig. 2. Our study of noise-induced gain control, in concert with recent studies of noise-coded signals (i.e. of coding signals into both drift and diffusion terms of Langevin equations—Lindner and Schimansky-Geier, 2001; Lánský and Sacerdote, 2001; Silberberg et al., 2002 in preperation), point to the necessity of properly identifying the neuronal input signals and control signals and the behavior of their means and variances before reaching conclusions about signal scaling, thresholding and amplification.

It has recently been shown that the response of the firing rate of a neuron to an increase in the intensity of the noisy input is instantaneous, because the probability flux at the threshold is directly proportional to the noise intensity (Silberberg et al., 2002 in preperation; Lindner and Schimansky-Geier, 2001). This means that the f–I characteristic can adjust itself instantaneously to changes in the intensity of stochastic processes driving the membrane potential. As a consequence, one can expect that the noise-induced divisive gain control discussed here and elsewhere

(Doiron et al., 2001a; Chance et al., 2002) can operate virtually in real time, in the sense that the slope changes ought to rapidly follow the changes in the amount of inhibition received by the cell. In other words, a time-varying inhibition will result in a time-varying gain control. This is expected to be the case in particular in circuits where the inhibitory input is actually proportional to the firing activity of the cell performing the gain control. Such feedback is ubiquitous in the nervous system, and is present for example in the pyramidal cells of the weakly electric fish Apteronotus Leptorhynchus (Berman and Maler, 1999). Our future work will consider the joint effect of NID and feedback in the presence of both excitatory and inhibitory inputs.

Acknowledgements

This work was supported by NSERC Canada. We are grateful to Len Maler and Petr Lansky for useful discussions.

References

Berman, N.J., Maler, L., 1999. Neural architecture of the electrosensory lateral line lobe: adaptations for coincidence detection, a sensory searchlight and frequency-dependent adaptive filtering. J. Exp. Biol. 202, 1243–1253.

Brown, D., Feng, J., Feerick, S., 1999. Variability of firing of Hodgkin–Huxley and FitzHugh–Nagumo neurons with stochastic synaptic input. Phys. Rev. Lett. 82, 4731–4734.

Bulsara, A.R., Elston, T.C., Doering, C.R., Lowen, S.B., Lindenberg, K., 1996. Cooperative behavior in periodically driven noisy integrate-and-fire models of neuronal dynamics. Phys. Rev. E 53, 3958–3969.

Carandini, M., Heeger, D., 1994. Summation and division by neurons in primate visual cortex. Science 264, 1333–1336.

Chance, F.S., Abbott, L.F., Reyes, A.D., 2002. Gain modulation from background synaptic input. Neuron 35, 773–782.

Chialvo, D.R., Longtin, A., Muller-Gerkin, J., 1997. Stochastic resonance in neuronal ensembles. Phys. Rev. E 55, 1798–1808.

Doiron, B., Longtin, A., Berman, N.J., Maler, L., 2001a. Subtractive and divisive inhibition: effect of voltage-dependent inhibitory conductances and noise. Neural Comput. 13, 227–248.

Doiron, B., Longtin, A., Turner, R.W., Maler, L., 2001b. Model of gamma frequency burst discharge generated by conditional backpropagation. J. Neurophysiol. 86, 1523–1545.

Ermentrout, G.B., 1996. Type I membranes, phase resetting curves, and synchrony. Neural Comput. 8, 979–1001.

Holt, G., Koch, C., 1997. Shunting inhibition does not have a divisive effect on firing rates. Neural Comput. 9, 1001–1013.

Koch, C., 1999. Biophysics of Computation, Information Processing in Single Neurons. Oxford University Press, Oxford.

Lánská, V., Lánský, P., Smith, C.E., 1994. Synaptic transmission in a diffusion model for neural activity. J. Theor. Biol. 166, 393–406.

Lánský, P., Lánská, V., 1987. Diffusion approximation of the neuronal model with synaptic reversal potentials. Biol. Cybern. 56, 19–26.

Lánský, P., Sato, S., 1999. The stochastic diffusion models of nerve membrane depolarizations and interspike interval generation. J. Periph. Nerv. Syst. 4, 27–42.

Lánský, P., Sacerdote, L., 2001. The Ornstein–Uhlenbeck neuronal model with signal-dependent noise. Phys. Lett. A 285, 132–140.

Lindner, B., Schimansky-Geier, L., 2001. Transmission of noise coded versus additive signals through a neuronal ensemble. Phys. Rev. Lett. 86, 2934–2937.

Longtin, A., 2000. Adiabatic and non-adiabatic resonances in excitable systems. In: Stochastic Processes in Physics, Chemistry, and Biology, Lecture Notes in Physics, vol. 557. Springer, Berlin, pp. 172–181.

Nelson, M.E., 1994. A mechanism for neuronal gain control by descending pathways. Neural Comput. 6, 255–269.

Ricciardi, L., 1977. Diffusion Processes and Related Topics in Biology. Springer, Berlin.

Salinas, E., Thier, P., 2000. Gain modulation: a major computational principle of the central nervous system. Neuron 27, 15–21.

Silberberg, G., Bethge, M., Markram, H., Tsodyks, M., Pawelzik, K., 2002. Rapid signaling by variance in ensembles of neocortical neurons, in preparation.

Tuckwell, H.C., 1989. Stochastic Processes in the Neurosciences. CBMS-NSF Regional Conference Series in Applied Mathematics, vol. 56. Society for Industrial and Applied Mathematics, Philadelphia.

Yu, X., Lewis, E.R., 1989. Studies with spike initiators: linearization by noise allows continuous signal modulation in neural networks. IEEE Trans. Biomed. Eng. 36, 36–43.